Quantum Network Science: Linking Graph Structure to Entanglement Performance

Rawan AlMakinah, M. Abdullah Canbaz

AI in Complex Systems Laboratory
University at Albany, SUNY
ralmakinah@albany.edu, mcanbaz@albany.edu

Abstract

Quantum communication networks—the substrate of a future quantum Internet—demand analytical tools that account for entanglement, fidelity, and quantum-specific constraints absent from classical models. In this paper, we introduce the Quantum Network Science (QNS) framework that adapts core network metrics to the quantum setting through fidelity-, success-probability-, and capacity-aware weighting. We formalize centrality (including Quantum PageRank and continuous-time quantum-walk variants), community structure on entanglement graphs, and robustness/percolation with fidelity thresholds. The framework is validated via analytic motifs and controlled simulations on Erdős–Rényi, scale-free, and small-world topologies, as well as satellite-assisted versus fiber-only designs. Our results show that (i) fidelity weighting reorders structural importance and can reconnect networks that appear fragmented classically; (ii) heavy-tailed degree patterns improve tolerance to random failures but heighten vulnerability to targeted hub attacks; (iii) small-world shortcuts induced by long-range quantum links shrink path lengths; and (iv) overlapping "connected components" emerge from entanglement swapping, motivating revised connectivity baselines. We also discuss design implications—degree caps and hub hardening, link-type diversity, multipath routing, and buffering policies—and outline extensions to temporal and multilayer modeling that couple the quantum plane with its classical control layer. QNS thus offers a principled, measurement-oriented foundation for analyzing, comparing, and engineering resilient, high-capacity quantum networks.

Introduction

Network science provides a unifying framework for analyzing complex systems across disciplines by modeling real-world phenomena as graphs, where nodes represent agents and edges encode pairwise interactions (Serrano and Gómez 2019; Majhi, Perc, and Ghosh 2022; Albert, Jeong, and Barabási 2000; Ghavasieh and De Domenico 2022; Al Musawi, Roy, and Ghosh 2023). As a branch of this field, complex network analysis exposes the structure and dynamics of real systems, identifying critical nodes, key pathways, and vulnerabilities (Al Musawi, Roy, and Ghosh 2023). At the interface of network science and quantum physics, interest in quantum networks—including the emerging quantum Internet—stems from their promise of secure long-distance communication grounded in quantum mechanics (Biamonte, Faccin, and De Domenico 2019; Shi and Fang 2024; Ghavasieh and De Domenico 2022). Extending complex-network methods into the quantum regime advances our understanding of physical complexity: recent cross-disciplinary work applies these tools to entanglement and transport, while information physics motivates a quantum-inspired theory of complex systems (Biamonte, Faccin, and De Domenico 2019).

Despite this progress, a general framework that systematically lifts classical complexity concepts to the quantum domain remains open. Classical network metrics (e.g., robustness under attack) do not directly translate because quantum systems exhibit fidelity (Gu 2010), entanglement (Horodecki et al. 2009), and the no-cloning constraint (Nehoran and Zhandry 2023). Comprehensive studies that use network science to evaluate quantum-specific strengths and vulnerabilities under targeted attacks—or that feed quantum features back into network-science methodology—are still scarce. In this work, we use standard network-science metrics (e.g., centrality and modularity) to analyze and enhance quantum networks. We compare quantum and classical networks under targeted attacks and show how quantum features, particularly entanglement, can be exploited to design more resilient and efficient architectures. We propose a framework and simulation that integrates classical and quantum insights within a common network-science toolkit.

The structure of the paper is as follows: Section 2 provides a background and related work, Section 3 formalizes the QNS framework, Section 4 details methodology and case studies, and reports the experiential setup and results, Section 5 discusses implications and limitations, and Section 6 concludes with future directions.

Background and Related Work

Complex Quantum Networks

The field of complex quantum networks is extending classical network science into the quantum setting by treating edges as non-classical resources—typically entangled qubit pairs distributed over fiber, free space, or

satellites—coordinated by classical side channels for status signals, control messages, and entanglement swapping (Nokkala, Piilo, and Bianconi 2024; Harney and Pirandola 2022; Conti, Malaney, and Win 2024; de Forges de Parny et al. 2023). This view supports the study of degree distributions, clustering, shortest paths, and percolation under constraints specific to quantum information, including decoherence, the no-cloning principle, and measurement effects (Meng et al. 2023; Cuquet and Calsamiglia 2009; Bianconi, Rahmede, and Wu 2015; Hu et al. 2025; Schlosshauer 2019; Bužek and Hillery 1996). Several classical patterns appear to carry over: quantum network topologies can show scale-free statistics with heavy-tailed degree distributions and hubs, and simulations indicate that scale-free architectures keep working under random link or node failures longer than alternatives in noisy repeater settings (Coutinho et al. 2022a). However, this comes at a cost: scale-free layouts are highly vulnerable to targeted attacks on hubs. Disabling even a small fraction of high-degree repeater nodes can disconnect a significant portion of the network and sharply increase the end-to-end entanglement threshold (Zhang and Zhuang 2021)—an issue we acknowledge and emphasize in this work. Likewise, satellite-assisted photonic networks can display small-world behavior, with average path lengths that grow slowly with network size and physically distant cities becoming "near" in the graph sense—yet these short paths also concentrate traffic on high-betweenness nodes, so compromising or jamming a few such repeaters can impact many nodes at once (Brito et al. 2021).

Quantum connectivity also departs from classical intuition. Because multiple entangled pairs with distance-dependent fidelities can coexist on a single physical link and be reconfigured through entanglement swapping, quantum "connected components" defined by entanglement reach can overlap—distinct clusters may share nodes—something not possible in purely classical graphs (He et al. 2025). This overlap means that faults or adversarial actions on shared nodes can propagate across clusters, draining or corrupting entanglement resources in multiple regions simultaneously (Gyongyosi and Imre 2019). The classical control plane further enlarges the attack surface (e.g., denial-of-service on heralding channels, route poisoning, timing and measurement-device attacks), and physical-layer exploits such as detector blinding can degrade link fidelity even when eavesdropping is eventually detected (Navas-Merlo and Garcia-Escartin 2021). These realities motivate security-aware metrics—extensions of centrality and communicability that weight edges by channel capacity, fidelity decay, distillation cost, and exposure to adversarial deletion; quantum-walk and entanglement-assisted centralities that reflect coherent transport and multipartite state generation; and percolation frameworks that model targeted removals and routing-induced depletion ("path percolation")(Santra and Malinovsky 2021). As metropolitan testbeds scale from a few nodes to dozens, incorporating these adversarial considerations—via hub hardening, degree caps, multipath routing, and diversity in physical channels—will be essential for designing topologies that are both resource-efficient and resilient to attacks that could otherwise affect many nodes (Clayton, Wu, and Bhattacharjee 2024).

Centrality in Quantum Networks

Centrality measures identify important nodes or links in a network, but in quantum settings, "importance" must reflect coherent transport, noise, and the cost of creating or routing entanglement (Nokkala et al. 2025). Quantum PageRank extends the classical algorithm by replacing the random walk with a quantum walk (or a quantum–stochastic walk with tunable dephasing), yielding rankings that still elevate high-degree hubs while more clearly separating secondary hubs and breaking degeneracies among low-ranked nodes; this finer resolution has been shown on synthetic scale-free and directed graphs and persists over a range of damping parameters (Loke et al. 2015). Continuous-time quantum walks (CTQWs) support related definitions: time-averaged visit probabilities (via the average mixing matrix) and resolvent-based scores act as quantum analogues of eigenvector and Katz centrality and converge to their classical counterparts under strong dephasing or measurement (Godsil 2011). Proof-of-principle experiments with integrated photonic circuits have implemented CTQW-based centrality on small graphs, confirming that interference patterns produce rank orders that differ from classical walk dynamics (Izaac et al. 2017). Beyond walk-based metrics, entanglement-aware betweenness ranks nodes by their ability to sustain entanglement-swapping paths while accounting for fidelity decay and distillation cost, and capacity-weighted variants of PageRank/eigenvector centrality integrate secret-key rate or channel capacity as edge weights (Koutsopoulos 2024). These quantum-aware measures also surface risks: nodes with high quantum betweenness concentrate traffic and become single points of failure—targeted disruption of a few such repeaters can disconnect large regions even if random failures are tolerated (Satoh et al. 2018).

Modularity and Communities

Modularity captures community structure—dense connections within groups, sparse between groups—and in quantum networks, the natural substrate is an "entanglement graph" whose edge weights encode entanglement rate, fidelity, or key capacity (Faccin et al. 2014). Community detection on such weighted graphs can reveal functional modules (e.g., metro-scale clusters of high-rate links) that support low-latency entanglement distribution and localized error management, with performance validated by improved end-to-end key rates within modules (Mondal et al. 2024). Quantum-walk methods provide complementary tools: clustering nodes by similarity of CTQW time-averaged distributions, by quantum hitting-time distances, or by spectral embeddings of the average mixing matrix can recover communities that classical random-walk methods miss when interference localizes probability on substructures (Coutinho et al. 2017). Because entanglement can be multiplexed and reconfigured by swapping, communities may overlap; mixed-membership and link-community approaches are therefore appropriate, as are multilayer extensions that track time-varying channel quality across classical and quantum

control layers (Vieira, Xavier, and Evsukoff 2020). Strong modularity has benefits (parallelizable routing, fault isolation) but also creates vulnerabilities: bridges between modules become high-betweenness bottlenecks, so an attack or outage on a small number of inter-community nodes can impact many users at once (Shai et al. 2014). A QNS framework should therefore estimate modularity on the entanglement graph with a tunable resolution parameter, report overlapping communities, and pair structural outputs with operational tests (e.g., throughput under traffic and adversarial removal), ensuring that detected communities correspond to real gains in quantum communication performance and resilience (Ronhovde and Nussinov 2009).

Robustness and Percolation

Network robustness is the ability to maintain connectivity and function when components fail, but in quantum settings, "function" must include entanglement reach, end-to-end fidelity, and secret-key or Bell-pair generation rates (Coutinho et al. 2022b). We model a quantum network as a graph $\mathcal{G} = (V, E)$ with $n = |V|$. Each edge $e \in E$ has a survival probability $p_e \in [0, 1]$, a link fidelity $F_e \in [0, 1]$, and an optional capacity $c_e(F_{\min}) \geq 0$ tied to a target fidelity $F_{\min}$. A simple way to fold quality into percolation is via the effective occupancy $\pi_e(F_{\min}) = p_e, \Pr[F_e! \geq! F_{\min}]$. Connectivity for a pair (i, j) can then be summarized by the two-terminal reliability $R_{ij}(F_{\min}) = \Pr[i! \overset{F_{\min}}{\longleftrightarrow}! j]$, and averaging over all pairs gives the network-level connectivity probability $P_{\text{conn}}(p, F_{\min}) = \frac{2}{n(n-1)} \sum_{i<j} R_{ij}(F_{\min})$ under homogeneous tests with $p_e = p$. Long-range reach is captured by the expected giant-component fraction $G(p, F_{\min})$, with a percolation threshold $p_c(F_{\min})$ defined as the smallest p for which G remains positive at large n. Studies of noisy repeaters show an abrupt loss of the giant entangled component at $p = p_c$—a discontinuity driven by swapping success, distillation costs, and fidelity cutoffs—unlike the smoother transitions often seen classically. Topology matters: Under random failures, scale-free layouts tend to delay fragmentation; however, the flip side is pronounced fragility to targeted attacks, where removing a small set of high-degree or high-betweenness repeaters can disconnect many users at once and sharply raise the fidelity needed for end-to-end entanglement. Robustness also has an operational dimension: routing consumes stored entanglement ("path percolation"), and correlated outages (e.g., weather or eclipse windows for free-space/satellite links) can trigger cascades even when individual links are nominally healthy.

For a QNS evaluation, we recommend reporting a compact set of fidelity-aware metrics under fixed noise and topology assumptions: $P_{\text{conn}}(p, F_{\min})$ and $G(p, F_{\min})$ for static reach; a robustness index $\mathcal{R}(F_{\min}) = \int_0^1 G(p, F_{\min}), dp$ to summarize performance across the whole failure range; and targeted-removal stress tests that compare random deletions with removals ranked by degree or by quantum betweenness to bound worst-case outcomes. Because resilience ultimately concerns usable throughput, capacity should be tracked via s–t key rates; a practical upper bound is the min-cut $C^{\text{key}}st = \min S :, s \in S, , t \notin S \sum_{e \in \partial S} c_e(F_{\min})$, whose persistence under failures indicates robustness "in capacity" rather than connectivity alone. These measurements make design levers explicit: degree caps and hub hardening; diversity across fiber, free-space, and satellite links; multipath and disjoint-path routing; proactive buffering of high-fidelity pairs; and adaptive swapping policies that trade rate for resilience when failures concentrate load. Quantifying and comparing these effects helps pick topologies and controls that degrade gracefully—maintaining acceptable fidelity and reach under random losses—while limiting the blast radius of targeted attacks that could otherwise affect many nodes.

Proposed QNS Framework

We propose a quantitative framework that adapts and extends network-science metrics to quantum communication settings. Figure 1 illustrates the abstraction we use: end users (terminals at the periphery) connect through intermediate repeater/switch nodes and quantum-memory elements; directed blue links denote candidate quantum channels and associated classical signaling. We represent such a system as a graph $G_Q = (V, E_Q)$ whose vertices V are end nodes, repeaters, and memories, and whose edges E_Q are entanglement-capable links. Each edge (i, j) may carry attributes such as entanglement fidelity F_{ij}, success probability p_{ij}, generation rate r_{ij}, and an effective capacity c_{ij} (e.g., secret-key or Bell-pair rate). We use a weight $w_{ij} = f(F_{ij}, p_{ij}, r_{ij})$ to fold these into a single link score and define a node's quantum degree as $k_i^{(Q)} = \sum_{j:(i,j)\in E_Q} w_{ij}$, which reduces to the classical degree when $w_{ij} = 1$ for every present edge. This weighted representation is the substrate for all metrics that follow.

Centrality is computed on the entanglement graph to iden-

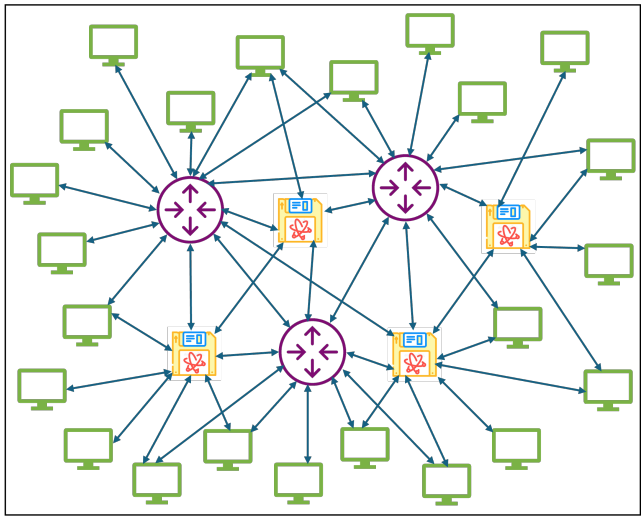

Figure 1: Sample quantum network topology used in the QNS framework. End users (periphery) connect through repeater/switch nodes and quantum-memory elements (interior). Blue arrows represent candidate quantum links with associated classical signaling.

tify important repeaters and memories. Classical measures (degree, betweenness, eigenvector/PageRank) are applied to the weighted graph to assess brokerage of entanglement-swapping paths and potential bottlenecks. In parallel, we include quantum-aware metrics: Quantum PageRank (a quantum-walk analogue of PageRank) that is known to separate secondary hubs and resolve low-rank degeneracies, and continuous-time quantum-walk (CTQW) centralities based on long-time average visit probabilities, which reflect coherent transport and the network spectrum. We benchmark all centralities against operational surrogates (e.g., impact on end-to-end key rate under load; failure impact when the node is removed) to verify that "high-centrality" aligns with components that matter for quantum communication.

Global topology metrics are extended in a fidelity-aware way. We study the degree distribution $P(k)$ under diverse designs (random, lattice, scale-free, small-world, satellite-assisted) and growth models to test for heavy tails and hub formation. Distances are evaluated both as unweighted hop counts and as weighted costs (e.g., $1/c_{ij}$ or functions of F_{ij} and p_{ij}). The average shortest-path length ℓ_{avg} and diameter are compared across designs; prior work suggests that long-range satellite links can induce small-world behavior by shrinking path lengths relative to fiber-only layouts. Clustering requires reinterpretation for entanglement: alongside the classical clustering coefficient computed on the entanglement graph, we use a quantum clustering $C_i^{(Q)}$ that counts neighbor pairs of i that are either directly entangled or can be made entangled via high-fidelity swapping through i (thresholded by $F_{\min}$).

Community structure is captured by modularity on the weighted entanglement graph. Using standard weighted modularity Q and algorithms such as Louvain or spectral methods, we detect groups with dense, high-quality links and sparse inter-group connectivity. Because entanglement can be multiplexed and reconfigured, communities may overlap; we therefore allow mixed-membership or link-community variants when needed. We then validate structural communities against performance by measuring whether intra-community routing achieves higher key rates or lower latency than inter-community routing, and by checking whether inter-community bridges are high-betweenness bottlenecks that merit protection.

Robustness and percolation are evaluated under comparable noise and topology assumptions. We track (i) pairwise connectivity via $R_{ij}(F_{\min}) = \Pr[i! \overset{F_{\min}}{\longleftrightarrow} !j]$, (ii) the network-level connectivity probability $P_{\text{conn}}(p, F_{\min}) = \frac{2}{n(n-1)} \sum_{i<j} R_{ij}(F_{\min})$, and (iii) the expected giant-component fraction $G(p, F_{\min})$ with threshold $p_c(F_{\min})$. Prior studies with realistic, noisy repeaters report an abrupt loss of the giant entangled component at $p = p_c$, in contrast with smoother classical transitions—a consequence of swapping success, purification cost, and fidelity cutoffs. We will compare random failures with targeted removals ranked by degree and by quantum betweenness to surface worst-case vulnerabilities, and we summarize performance across the whole failure range using a robustness index $\mathcal{R}(F_{\min}) = \int_0^1 G(p, F_{\min}), dp$. Because resilience ultimately concerns usable throughput, we complement connectivity metrics with capacity min-cuts, reporting the persistence of s–t key-rate bounds $C^{\text{key}}st = \min S :, s \in S, , t \notin S \sum_{(i,j)\in\partial S} c_{ij}$ under failures and attacks. Finally, we run simulation experiments across the aforementioned topologies with realistic link models (loss, decoherence, weather for free-space/satellite links) and traffic patterns to generate comparative scorecards. These outputs guide design levers—degree caps and hub hardening, diversity across fiber/free-space/satellite links, multipath and disjoint-path routing, proactive buffering of high-fidelity pairs, and adaptive swapping policies—so that engineered networks deliver small-world reach and high capacity while limiting the blast radius of targeted attacks.

Methodology and Case Studies

To demonstrate the QNS framework, we couple lightweight analytic modeling with controlled simulation studies on representative topologies and evaluate both classical and quantum-aware metrics side by side.

Experimental Setup

We model each network as a graph $G_Q = (V, E_Q)$ with $|V| = N$. "Classical" analyses use the unweighted adjacency; "quantum" analyses use an *entanglement graph* whose edge weights encode link quality. Unless noted, we take a simple fidelity-aware weight $w_{ij} = F_{ij} \in [0, 1]$ (or $w_{ij} = p_{ij}F_{ij}$ when success probability p_{ij} is modeled), and we optionally threshold at $F_{\min}$ to decide if a link is usable. Metrics are then computed on the same underlying topology, once classically and once on the fidelity-weighted version, to isolate the effect of quantum constraints.

We study three canonical topologies with $N = 30$ nodes: Erdős–Rényi random (ER), Barabási–Albert scale-free (BA), and Watts–Strogatz small-world (WS). For ER we select edges with probability p to yield the edge counts shown in the results; BA uses preferential attachment (2–3 edges per arriving node) to induce hubs; WS starts from a ring with k nearest neighbors and rewiring probability β to add shortcuts. The bottom row of Fig. 2 applies the same topologies but assigns synthetic link fidelities (drawn from a mild heterogeneous distribution) to produce a fidelity-weighted view. Node sizes reflect degree (classical) or weighted degree $k_i^{(Q)} = \sum_j w_{ij}$ (quantum), and colors illustrate communities returned by a standard modularity maximizer.

We consider two failure regimes. (i) *Link failures:* a 25% random bond failure is applied uniformly to both the classical and quantum views, after which metrics are recomputed. (ii) *Single node failure:* one random node (and its incident edges) is removed; we then recompute all metrics. For both regimes, we report connectivity, centrality (degree, PageRank, eigenvector, betweenness), clustering, transitivity, assortativity, clique counts, community count, modularity, and, for the quantum view, the average link fidelity. The visualization summarizing the three topologies (classical on top, fidelity-weighted on bottom) is shown in Fig. 2.

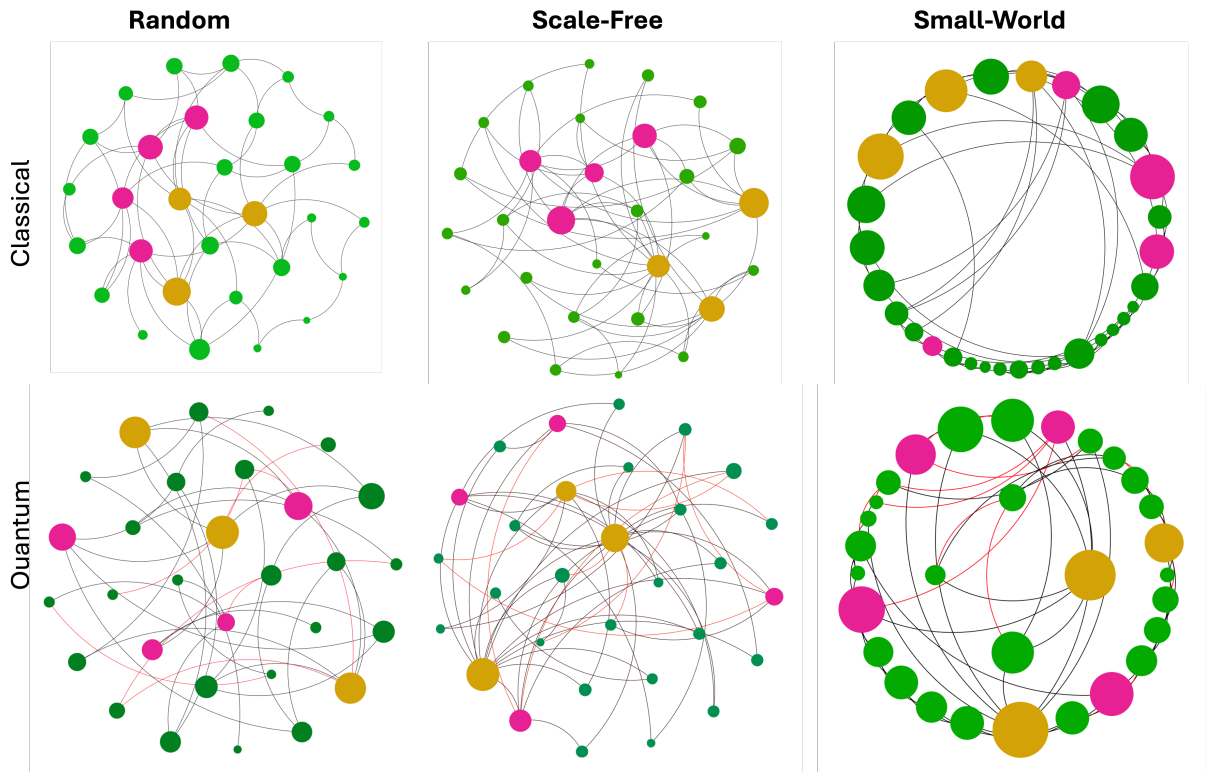

Figure 2: Visual comparison across topologies. **Top:** classical (unweighted) ER, BA, and WS graphs. **Bottom:** same graphs with edges weighted by simulated link fidelities ("quantum" view). Node size scales with (weighted) degree; node color indicates detected communities.

Metric	**Random**		**Scale-Free**		**Small-World**	
	Classical	Quantum	Classical	Quantum	Classical	Quantum
Total Nodes	30	30	30	30	30	30
Total Edges	47	47	56	56	60	60
Failed Edges	11	11	14	14	15	15
Functional Edges	36	36	42	42	45	45
Connected Components	2	1	1	1	1	1
Largest Component Size	29	30	30	30	30	30
Fully Connected	No	Yes	Yes	Yes	Yes	Yes
Average Degree Centrality	0.11	0.11	0.13	0.13	0.14	0.14
Average PageRank	0.03	0.03	0.03	0.03	0.03	0.03
Average Eigenvector Centrality	0.15	0.15	0.15	0.16	0.15	0.18
Average Betweenness Centrality	0.06	0.08	0.05	0.05	0.07	0.09
Average Clustering Coefficient	0.14	0.17	0.40	0.37	0.41	0.40
Transitivity	0.10	0.16	0.19	0.16	0.39	0.39
Assortativity	-0.11	-0.15	-0.30	-0.35	-0.20	-0.08
Number of Cliques	39	36	35	37	32	31
Total Communities	5	6	3	5	4	4
Modularity	0.42	0.52	0.34	0.36	0.56	0.56
Average Fidelity	–	0.65	–	0.66	–	0.63

Table 1: Comparison of classical and quantum network metrics across topologies (link failure rate = 0.25).

Experimental Results

Tables 1 and 2 summarize the side-by-side metrics for the 25% link-failure regime and for the single-node failure regime, respectively. Values correspond to a representative seeded run; repeated trials show the same qualitative trends.

Metric	Random		Scale-Free		Small-World	
	Classical	Quantum	Classical	Quantum	Classical	Quantum
Total Nodes	30	30	30	30	30	30
Functional Nodes	29	29	29	29	29	29
Failed Nodes	1	1	1	1	1	1
Total Edges	46	36	56	56	60	60
Failed Edges	4	5	2	7	4	12
Functional Edges	42	31	54	49	56	48
Connected Components	1	2	1	1	1	1
Largest Component Size	29	28	29	29	29	29
Fully Connected	Yes	No	Yes	Yes	Yes	Yes
Average Degree Centrality	0.10	0.08	0.13	0.13	0.14	0.14
Average PageRank	0.03	0.03	0.03	0.03	0.03	0.03
Average Eigenvector Centrality	0.15	0.13	0.16	0.16	0.17	0.16
Average Betweenness Centrality	0.07	0.09	0.05	0.05	0.07	0.09
Average Clustering Coefficient	0.14	0.08	0.23	0.24	0.33	0.42
Transitivity	0.12	0.13	0.18	0.13	0.33	0.42
Assortativity	-0.26	-0.02	-0.15	-0.31	-0.07	0.05
Number of Cliques	34	29	38	40	33	31
Total Communities	5	6	6	5	5	4
Modularity	0.48	0.56	0.36	0.37	0.50	0.55
Average Fidelity	–	0.78	–	0.83	–	0.79

Table 2: Comparison of classical and quantum network metrics across topologies after one node failure.

Baseline with 25% link failures (Table 1): The ER graph illustrates how fidelity weighting can "stitch" a network that is classically split: the classical view has two components and is not fully connected, whereas the fidelity-weighted view remains in a single component and is fully connected. The gain coincides with higher transitivity and modularity, suggesting that a few stronger links bridge otherwise weakly connected regions. In BA, both views remain fully connected; eigenvector centrality rises slightly in the quantum view (0.16 vs 0.15), indicating that influence concentrates on a subset of high-fidelity hub neighborhoods, while clustering/transitivity fall modestly, consistent with hub-centric structure. For WS, quantum weighting increases eigenvector and betweenness averages, highlighting shortcut nodes that carry high-quality long-range links; assortativity moves toward neutral (from -0.20 to -0.08), indicating a less degree-correlated interaction pattern once link quality is considered. Across all topologies, modularity either matches or increases under the quantum view, reflecting clearer community boundaries when weak links are down-weighted.

Single node failure (Table 2): ER shows the expected sensitivity when the removed node is fidelity-critical: the quantum view splits into two components and loses more functional edges (31 vs 42 classically), with clustering dropping from 0.14 to 0.08. The jump in modularity (0.48 to 0.56) and the near-zero assortativity indicate a reorganization into tighter, more homogeneous modules after the cut—useful diagnostically for identifying bridge nodes that merit hardening. BA remains fully connected in both views, but the quantum view loses more edges (49 vs 54), consistent with hub-adjacent links being quality-limited; nonetheless, centrality averages are stable, showing classic scale-free resilience to a random single-node fault. WS is robust and even shows increased local cohesion in the quantum view (clustering and transitivity both rise to 0.42), a hallmark of small-worlds where many alternative short paths persist. In all three, betweenness in the quantum view is higher than or equal to classical, flagging critical repeaters that concentrate viable entanglement-swapping routes.

Takeaways for QNS. Fidelity-aware weighting changes both structure and function: it can (i) reconnect networks that appear fragmented classically, (ii) re-rank "bridge" nodes via betweenness/eigenvector gains, and (iii) sharpen community structure. Under failures, ER is sensitive to the loss of fidelity-critical bridges, BA is robust to random single faults but will be fragile to targeted hub removal (as shown elsewhere in the paper), and WS retains graceful degradation thanks to redundant shortcuts. These patterns validate the QNS choice to pair classical metrics with fidelity-aware counterparts and to evaluate both connectivity and capacity-oriented resilience under shared failure models.

Conclusion: Outlook and Future Directions

In this work, we present a Quantum Network Science (QNS) framework that carries core ideas from network theory into the quantum regime and makes them operational for design and evaluation. By reformulating centrality, modularity, and robustness with fidelity-, success-probability-, and capacity-aware weights, the framework exposes structural regularities and fragilities that are invisible to classical analyses. Our case studies indicate that heavy-tailed degree patterns can improve tolerance to random failures while concentrat-

ing risk under targeted attacks; that quantum PageRank and CTQW-based centralities surface secondary hubs and bridge nodes relevant for entanglement routing; and that quantum-specific structures—such as overlapping connected components induced by swapping and multiplexed entanglement—require revised connectivity notions and percolation baselines. These results translate into practical guidance on topology selection (e.g., controlled hub formation with degree caps), repeater placement and hardening, multipath routing, and buffering policies that preserve end-to-end fidelity under stress.

Looking ahead, QNS can evolve from a descriptive toolkit into a prescriptive, closed-loop design methodology. First, *dynamic QNS* is necessary: real networks are time-varying as links are established, distilled, consumed, and refreshed. Extending metrics to temporal graphs and evaluating time-to-entanglement, burstiness, and environmental effects (e.g., weather windows for free-space channels) will enable performance envelopes and service-level guarantees, not just static scorecards. Coupling temporal metrics with online control—adaptive swapping, re-routing, and proactive pair buffering—points to *digital twins* that forecast failures and recommend control actions in real time.

Second, *multilayer QNS* should co-model the classical control plane and the quantum plane as coupled layers. Metrics that jointly assess classical signaling latency, route consistency, and attack surface alongside quantum capacities will better predict end-to-end behavior. Security-aware variants—targeted removal by quantum betweenness, adversarial percolation with correlated faults, and control-plane denial-of-service models—can quantify blast radii and guide defense-in-depth (hub hardening, link diversity, and disjoint-path provisioning).

Third, *experimental validation and benchmarking* must accompany deployments. We propose standardized QNS benchmark suites: metropolitan testbeds and satellite–ground hybrids with public link-quality traces; reference tasks (key-rate maximization at target fidelity, outage-constrained routing); and reproducible pipelines that compute both classical and quantum-aware metrics from raw logs. A shared corpus would enable rigorous comparison of algorithms and topologies under matched conditions.

Fourth, *integration with protocol performance* should be routine. Structural signals ought to predict operational outcomes such as secret-key throughput, entanglement distribution rate, latency to GHZ-state formation, and reliability at threshold $F_{\min}$. Calibrated mappings from QNS metrics (e.g., quantum betweenness, capacity min-cuts, modularity) to protocol-level KPIs, validated on hardware-in-the-loop experiments, would support multi-objective optimization over cost, capacity, latency, and resilience.

Finally, several theoretical directions remain open: universality classes for quantum percolation (continuous vs. discontinuous transitions), scaling laws for ℓ_{avg} under fidelity-aware shortcuts, limit theorems for quantum-walk centralities on random graphs, and conditions under which overlapping entanglement components guarantee global reach despite local fragility (Nath and Roy 2025). Addressing these questions will tighten the link between abstract models and engineered networks.

Please note that the quantum realm of networking is an ocean; our contribution is to light a narrow, navigable channel toward quantitative design and control of quantum networks. QNS provides a rigorous lens for reasoning about—and ultimately steering—the quantum internet by unifying structural diagnostics, adversarial stress tests, and protocol-level performance. The framework supports standardization, prioritizes infrastructure investments, and enables adaptive control that responds to failures and demand in real time. While our initial focus was on undirected abstractions and single-node failures to establish conceptual clarity, future work will extend QNS to directed quantum networks, where asymmetry in links and capacities may yield qualitatively different resilience patterns. Similarly, we plan to generalize from single-node disruptions to broader classes of failures—including edge removals, correlated multi-node attacks, and cascading effects—allowing the framework to capture a richer set of real-world stressors. As testbeds scale from a few nodes to city- and nation-scale fabrics, QNS is positioned to serve as both the measurement language and the design compass for resilient high-capacity quantum communication networks.

Appendix

Glossary of Network Metrics in Quantum Networks Visualized on Sample Quantum Network Topology (Figure 3)

Nodes. Individual entities (end users, repeaters, memories) that participate in distributing or storing entanglement and form the substrate of distributed quantum information processing (Lu et al. 2020).

Edges. Connections between nodes corresponding to quantum or classical communication links; in the quantum view, edges often carry attributes such as success probability, fidelity, or key/entanglement rate (Ouyang et al. 2018).

Connected components. Maximal sets of nodes within which every pair is mutually reachable; in the entanglement graph, this reflects paths that meet a target fidelity threshold (Aharonov 2000).

Largest component size. The order of the largest connected component (the "giant component") and a standard order parameter for connectivity/percolation analyses (Elumar, Sood, and Yağan 2023).

Degree centrality. A node-importance score based on the number (or weight) of its incident edges; in quantum settings, degree may be fidelity- or capacity-weighted (Zhang and Luo 2017).

PageRank. A centrality for directed graphs is defined as the stationary distribution of a damped random walk on the network; for undirected graphs, it reduces to a closely related stochastic ranking over bidirectional edges (Pinheiro 2022).

Eigenvector centrality. A spectral centrality that assigns a high score to nodes connected to other high-scoring nodes, generalizing degree to account for neighbor influence (Pinheiro 2022).

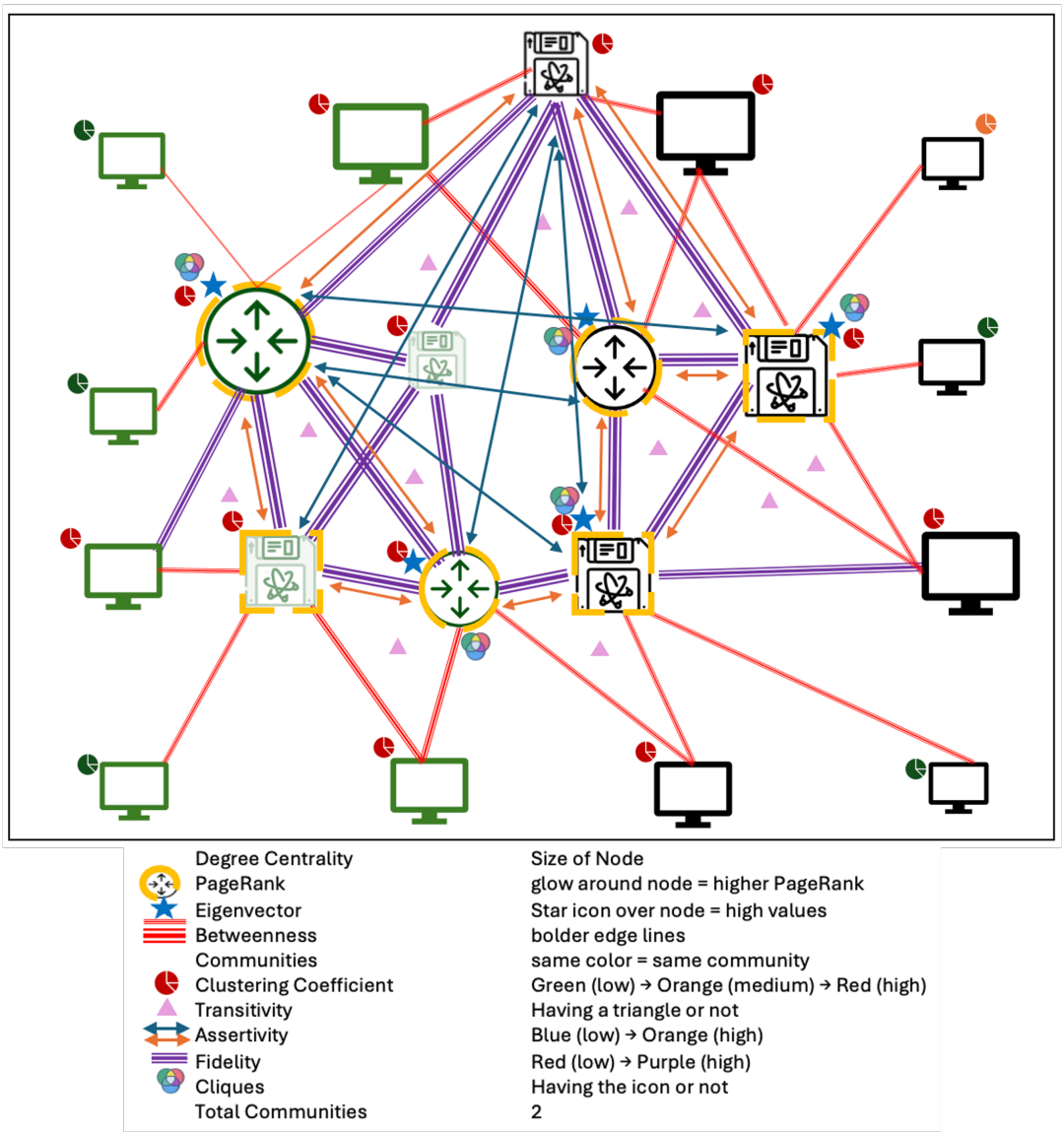

Figure 3: Appendix B: Network Metrics Visualized on Sample Quantum Network Topology

Betweenness centrality. The fraction of all-pairs shortest paths that pass through a node, capturing brokerage and potential bottlenecks for information (or entanglement) flow (Zhang and Luo 2017).

Clustering coefficient. The tendency of a node's neighbors to be mutually connected (local clustering) or, in quantum variants, the propensity for neighbor pairs to be directly or swap-enabled entangled (Watts and Strogatz 1998).

Transitivity. The global clustering coefficient: three times the number of triangles divided by the number of connected triples, providing a network-level measure of triadic closure (Vasques Filho and O'Neale 2020).

Assortativity. Degree–degree (or attribute-based) correlation across edges; positive values indicate like-with-like connectivity, while negative values indicate disassortative mixing (Noldus and Van Mieghem 2015).

Number of cliques. The count of complete subgraphs present in the network, often used to quantify dense mesoscale structure (Mokken et al. 1979).

Community. A subset of nodes more densely connected internally than externally; in quantum networks, communities may reflect regions with abundant high-quality entanglement (Radicchi et al. 2004).

Modularity. A quality function that scores a partition by comparing observed intra-community edge weight to a null-model expectation; higher values indicate sharper community structure (Ghalmane et al. 2019).

Fidelity. A similarity measure between quantum states; for channels, average state fidelity quantifies how well the channel preserves quantum information and serves as a link-quality indicator in entanglement graphs (Liang et al. 2019).

References

Aharonov, D. 2000. Quantum to classical phase transition in noisy quantum computers. *Physical Review A*, 62(6): 062311.

Al Musawi, A. F.; Roy, S.; and Ghosh, P. 2023. Examining indicators of complex network vulnerability across diverse attack scenarios. *Scientific Reports*, 13(1): 18208.

Albert, R.; Jeong, H.; and Barabási, A.-L. 2000. Error and attack tolerance of complex networks. *nature*, 406(6794): 378–382.

Biamonte, J.; Faccin, M.; and De Domenico, M. 2019. Complex networks from classical to quantum. *Communications Physics*, 2(1): 53.

Bianconi, G.; Rahmede, C.; and Wu, Z. 2015. Complex quantum network geometries: Evolution and phase transitions. *Physical Review E*, 92(2): 022815.

Brito, S.; Canabarro, A.; Cavalcanti, D.; and Chaves, R. 2021. Satellite-based photonic quantum networks are small-world. *Prx Quantum*, 2(1): 010304.

Bužek, V.; and Hillery, M. 1996. Quantum copying: Beyond the no-cloning theorem. *Physical Review A*, 54(3): 1844.

Clayton, C.; Wu, X.; and Bhattacharjee, B. 2024. Efficient Routing on Quantum Networks using Adaptive Clustering. arXiv:2410.23007.

Conti, A.; Malaney, R.; and Win, M. Z. 2024. Satellite-terrestrial quantum networks and the global quantum internet. *IEEE Communications Magazine*, 62(10): 34–39.

Coutinho, B. C.; Munro, W. J.; Nemoto, K.; and Omar, Y. 2022a. Robustness of noisy quantum networks. *Communications Physics*, 5(1): 105.

Coutinho, B. C.; Munro, W. J.; Nemoto, K.; and Omar, Y. 2022b. Robustness of noisy quantum networks. *Communications Physics*, 5(1).

Coutinho, G.; Godsil, C.; Guo, K.; and Zhan, H. 2017. A New Perspective on the Average Mixing Matrix. arXiv:1709.03591.

Cuquet, M.; and Calsamiglia, J. 2009. Entanglement percolation in quantum complex networks. *Physical review letters*, 103(24): 240503.

de Forges de Parny, L.; Alibart, O.; Debaud, J.; Gressani, S.; Lagarrigue, A.; Martin, A.; Metrat, A.; Schiavon, M.; Troisi, T.; Diamanti, E.; et al. 2023. Satellite-based quantum information networks: use cases, architecture, and roadmap. *Communications Physics*, 6(1): 12.

Elumar, E. C.; Sood, M.; and Yağan, O. 2023. On the robustness, connectivity and giant component size of random K-out graphs. *arXiv preprint arXiv:2311.02319*.

Faccin, M.; Migdał, P.; Johnson, T. H.; Bergholm, V.; and Biamonte, J. D. 2014. Community detection in quantum complex networks. *Physical Review X*, 4(4): 041012.

Ghalmane, Z.; El Hassouni, M.; Cherifi, C.; and Cherifi, H. 2019. Centrality in modular networks. *EPJ Data Science*, 8(1): 15.

Ghavasieh, A.; and De Domenico, M. 2022. Statistical physics of network structure and information dynamics. *Journal of Physics: Complexity*, 3(1): 011001.

Godsil, C. 2011. Average mixing of continuous quantum walks. arXiv:1103.2578.

Gu, S.-J. 2010. Fidelity approach to quantum phase transitions. *International Journal of Modern Physics B*, 24(23): 4371–4458.

Gyongyosi, L.; and Imre, S. 2019. Adaptive routing for quantum memory failures in the quantum internet. *Quantum Information Processing*, 18(2): 52.

Harney, C.; and Pirandola, S. 2022. Analytical methods for high-rate global quantum networks. *PRX Quantum*, 3(1): 010349.

He, B.; Loke, S. W.; Lu, L.; and Zhang, D. 2025. Efficient Entanglement Swapping in Quantum Networks for Multi-User Scenarios. *Entropy*, 27(6): 615.

Horodecki, R.; Horodecki, P.; Horodecki, M.; and Horodecki, K. 2009. Quantum entanglement. *Reviews of modern physics*, 81(2): 865–942.

Hu, X.; Dong, G.; Christensen, K.; Sun, H.; Fan, J.; Tian, Z.; Gao, J.; Havlin, S.; Lambiotte, R.; and Meng, X. 2025. Unveiling the importance of nonshortest paths in quantum networks. *Science advances*, 11(9): eadt2404.

Izaac, J. A.; Zhan, X.; Bian, Z.; Wang, K.; Li, J.; Wang, J. B.; and Xue, P. 2017. Centrality measure based on continuous-time quantum walks and experimental realization. *Phys. Rev. A*, 95: 032318.

Koutsopoulos, I. 2024. Optimal Fidelity-Aware Entanglement Distribution in Linear Quantum Networks. arXiv:2407.09171.

Liang, Y.-C.; Yeh, Y.-H.; Mendonça, P. E.; Teh, R. Y.; Reid, M. D.; and Drummond, P. D. 2019. Quantum fidelity measures for mixed states. *Reports on Progress in Physics*, 82(7): 076001.

Loke, T.; Tang, J. W.; Rodriguez, J.; Small, M.; and Wang, J. B. 2015. Comparing classical and quantum PageRanks. arXiv:1511.04823.

Lu, H.; Huang, C.-Y.; Li, Z.-D.; Yin, X.-F.; Zhang, R.; Liao, T.-L.; Chen, Y.-A.; Li, C.-M.; and Pan, J.-W. 2020. Counting classical nodes in quantum networks. *Physical review letters*, 124(18): 180503.

Majhi, S.; Perc, M.; and Ghosh, D. 2022. Dynamics on higher-order networks: A review. *Journal of the Royal Society Interface*, 19(188): 20220043.

Meng, X.; Hu, X.; Tian, Y.; Dong, G.; Lambiotte, R.; Gao, J.; and Havlin, S. 2023. Percolation theories for quantum networks. *Entropy*, 25(11): 1564.

Mokken, R. J.; et al. 1979. Cliques, clubs and clans. *Quality & Quantity*, 13(2): 161–173.

Mondal, M. S.; Fields, D.; Malinovsky, V. S.; and Santra, S. 2024. Entanglement topography of large-scale quantum networks. arXiv:2312.16009.

Nath, D.; and Roy, S. 2025. General Concurrence Percolation on Quantum Networks. *arXiv preprint arXiv:2501.11004*.

Navas-Merlo, C.; and Garcia-Escartin, J. C. 2021. Detector blinding attacks on counterfactual quantum key distribution. *Quantum Information Processing*, 20(6).

Nehoran, B.; and Zhandry, M. 2023. A computational separation between quantum no-cloning and no-telegraphing. *arXiv preprint arXiv:2302.01858*.

Nokkala, J.; Piilo, J.; and Bianconi, G. 2024. Complex quantum networks: a topical review. *Journal of Physics A: Mathematical and Theoretical*, 57(23): 233001.

Nokkala, J.; Piilo, J.; Meena, C.; et al. 2025. Stability of Continuous Time Quantum Walks in Complex Networks. *arXiv preprint arXiv:2507.17880*.

Noldus, R.; and Van Mieghem, P. 2015. Assortativity in complex networks. *Journal of complex networks*, 3(4): 507–542.

Ouyang, B.; Xia, Y.; Wang, C.; Ye, Q.; Yan, Z.; and Tang, Q. 2018. Quantifying importance of edges in networks. *IEEE Transactions on Circuits and Systems II: Express Briefs*, 65(9): 1244–1248.

Pinheiro, C. A. R. 2022. *Network science: Analysis and optimization algorithms for real-world applications*. John Wiley & Sons.

Radicchi, F.; Castellano, C.; Cecconi, F.; Loreto, V.; and Parisi, D. 2004. Defining and identifying communities in networks. *Proceedings of the national academy of sciences*, 101(9): 2658–2663.

Ronhovde, P.; and Nussinov, Z. 2009. Multiresolution community detection for megascale networks by information-based replica correlations. *Physical Review E—Statistical, Nonlinear, and Soft Matter Physics*, 80(1): 016109.

Santra, S.; and Malinovsky, V. S. 2021. Quantum networking with short-range entanglement assistance. *Physical Review A*, 103(1).

Satoh, T.; Nagayama, S.; Oka, T.; and Van Meter, R. 2018. The network impact of hijacking a quantum repeater. *Quantum Science and Technology*, 3(3): 034008.

Schlosshauer, M. 2019. Quantum decoherence. *Physics Reports*, 831: 1–57.

Serrano, D. H.; and Gómez, D. S. 2019. Centrality measures in simplicial complexes: applications of TDA to Network Science. *arXiv preprint arXiv:1908.02967*.

Shai, S.; Kenett, D.; Kenett, Y.; Faust, M.; Dobson, S.; and Havlin, S. 2014. Resilience of modular complex networks. arXiv.

Shi, R.-h.; and Fang, X.-q. 2024. Anonymous classical message transmission through various quantum networks. *IEEE Transactions on Network Science and Engineering*, 11(3): 2901–2913.

Vasques Filho, D.; and O'Neale, D. R. 2020. Transitivity and degree assortativity explained: The bipartite structure of social networks. *Physical Review E*, 101(5): 052305.

Vieira, V. d. F.; Xavier, C. R.; and Evsukoff, A. G. 2020. A comparative study of overlapping community detection methods from the perspective of the structural properties. *Applied Network Science*, 5(1): 51.

Watts, D. J.; and Strogatz, S. H. 1998. Collective dynamics of 'small-world'networks. *nature*, 393(6684): 440–442.

Zhang, B.; and Zhuang, Q. 2021. Quantum internet under random breakdowns and intentional attacks. *Quantum Science and Technology*, 6(4): 045007.

Zhang, J.; and Luo, Y. 2017. Degree centrality, betweenness centrality, and closeness centrality in social network. In *2017 2nd international conference on modelling, simulation and applied mathematics (MSAM2017)*, 300–303. Atlantis press.